JMEPEG (2004) 13:593-599
DOI: 10.1361/15477020420828

1059-9495/$19.00

Relationship Between Ultrasonic Characteristics and Mechanical Properties of Tempered Martensitic Stainless Steel

Cheng-Hsun Hsu, Hwei-Yuan Teng, and Yeong-Jern Chen

(Submitted January 21, 2004)

This research studied the relationship between the ultrasonic characteristics and the mechanical properties of tempered CA-15 martensitic stainless steel (MSS). The results show that, for as-quenched specimens, a chromium carbide film at the martensitic boundary of the as-cast specimen will disappear causing a change in the mechanical properties (e.g., the tensile strength is decreased or the hardness and the toughness are increased). For the tempered MSS, the correlation of the ultrasonic velocity and the tensile strength, hardness, and toughness is not obvious. However, there is a highly positive correlation with the elastic modulus (*E*) of the material. For the ultrasonic attenuation evaluation, the attenuation coefficient (α) has a positive correlation with the tensile strength and the hardness, while there is a negative correlation with the toughness and the elongation. Also, a higher-frequency probe would cause the better sensitivity, but the data are relatively dispersed.

Keywords attenuation coefficient, mechanical property, tempered martensitic stainless steel, ultrasonic velocity

1. Introduction

Martensitic stainless steel (MSS) possesses excellent high-temperature strength and corrosion resistance and is widely used in highly stressed parts, such as turbines and gas distributor heads.[1] In general, MSS needs to be heat treated by austenitizing and tempering processes to achieve the desirable mechanical and corrosion properties. Ultrasonic techniques are used not only to detect discontinuities, such as voids, cracks, inclusions, and precipitates,[2-5] but are also used to evaluate such characteristics of a material as microstructure, grain size, and residual stress.[6-10] The velocity and attenuation of sound waves are commonly used for such purposes.

The velocity of an ultrasonic wave as it propagates through a solid material is affected by the elastic modulus (E), the density (ρ), and Poisson's ratio (μ). The relationships among these properties and the longitudinal or transverse velocity of the ultrasonic wave (i.e., V_L or V_T, respectively) can be expressed as follows[11]:

$$V_L = \sqrt{\frac{E(1-\mu)}{\rho(1+\mu)(1-2\mu)}} \quad \text{(Eq 1)}$$

$$V_T = \sqrt{\frac{E}{2\rho(1+\mu)}} \quad \text{(Eq 2)}$$

Cheng-Hsun Hsu, Department of Materials Engineering Tatung University, Taipei, Taiwan 104, Republic of China; and **Hwei-Yuan Teng,** and **Yeong-Jern Chen,** Department of Mechanical Engineering, De Lin Institute of Technology, Tu-Cheng, Taiwan 236, Republic of China. Contact e-mail: chhsu@ttu.edu.tw.

Equations 1 and 2 imply that the acoustic speed is a constant value and thus is characteristic of a material in a specific state. That is to say, a microstructural change in the material can cause an alteration of the ultrasonic velocity.

When an ultrasonic wave travels through a solid object, its amplitude (A) or its intensity (I) will decay exponentially with respect to the distance (X) of the sound propagation.[11] The relationship can be written as

$$A = A_o \exp(-\alpha X), \text{ or } I = I_o \exp(-\alpha X) \quad \text{(Eq 3)}$$

where A_o and I_o are the initial sound amplitude and the intensity, respectively. The attenuation coefficient (α) can be further described by[2,11]

$$\alpha(f) = \frac{20[\log(A1/A2) + 2\log R]}{2d} \quad \text{(Eq 4)}$$

where $\alpha(f)$ is in decibels per millimeter, $A1$ and $A2$ are peak amplitudes of the first and second transmitted pulses in millimeters, and d is the test specimen thickness in millimeters. The term R, the reflection coefficient of the coupling plane, is equal to $(1 - \eta)/(1 + \eta)$, and η is the acoustic impedance of the

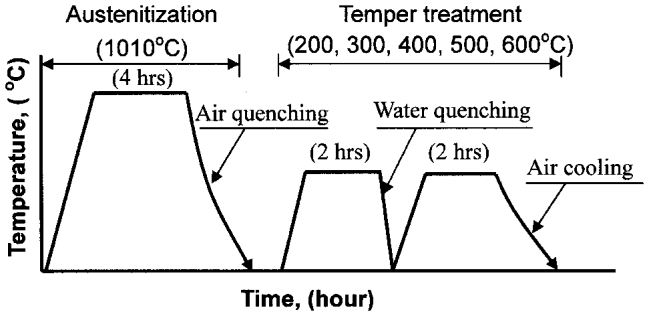

Fig. 1 Heat treatment conditions in this experiment

coupling plane. The attenuation coefficient of the ultrasonic wave is affected by absorption (i.e., influenced by dislocation damping, magnetic resistance, and thermal elasticity) and scattering (i.e., influenced by grain boundaries, voids, inclusions, second-phase particles, and cracks).[8] The attenuation coefficient is also a function of detector frequency.

It is important to understand the relationships between the ultrasonic characteristics (velocity and attenuation) and the mechanical properties of MSS, tempered at various temperatures such that the mechanical properties of the material can be evaluated by nondestructive ultrasonic techniques.

2. Experimental Procedure

2.1 Material and Heat Treatment

In this study, 32 mm thick, CA-15-cast MSS plates produced by a regular foundry were used as the experimental material. The chemical composition (wt.%) of the material was

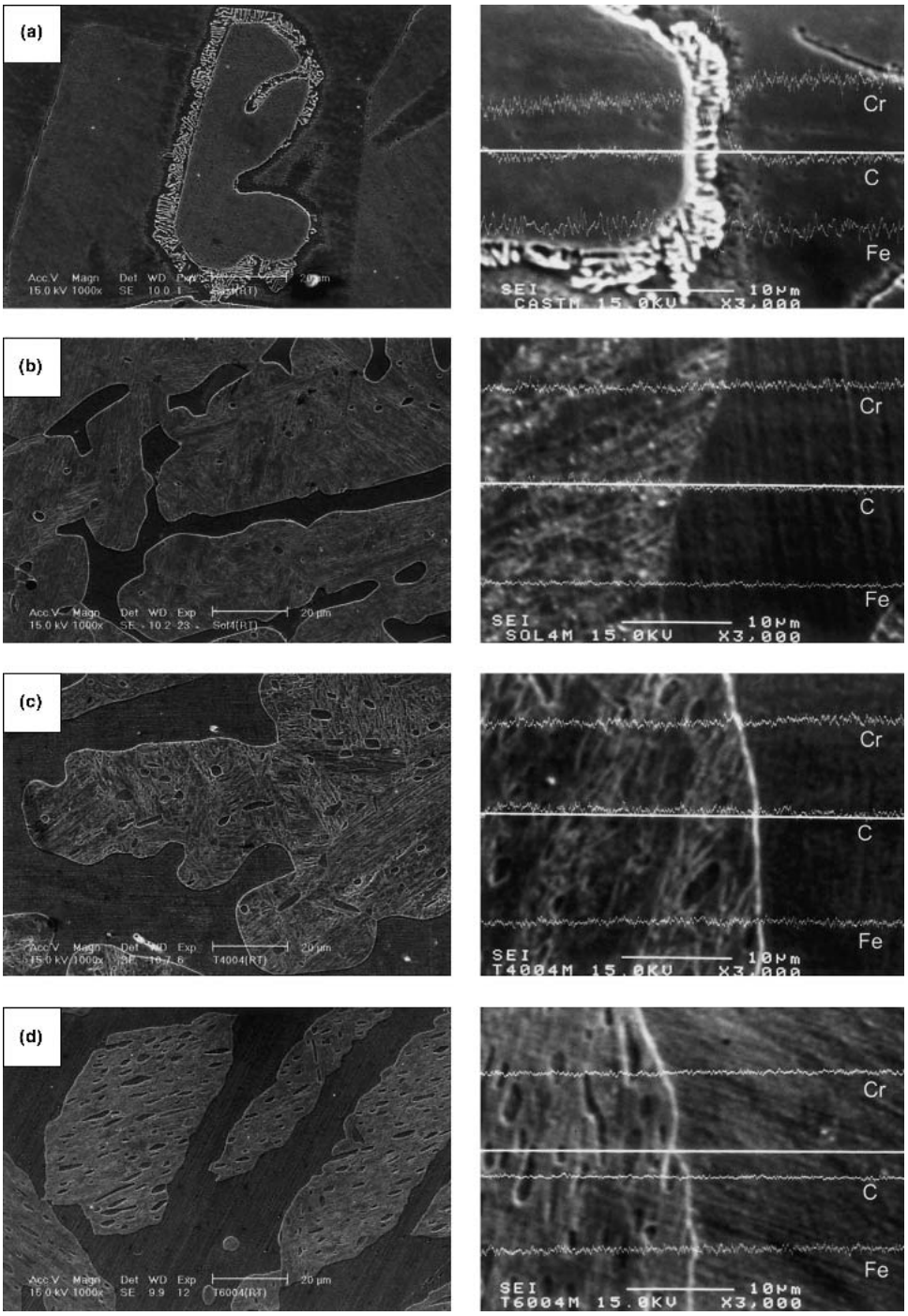

Fig. 2 SEM and EPMA scan of the experimental material: **(a)** as-cast; **(b)** as-quenched; **(c)** tempered at 400 °C; and **(d)** tempered at 600 °C

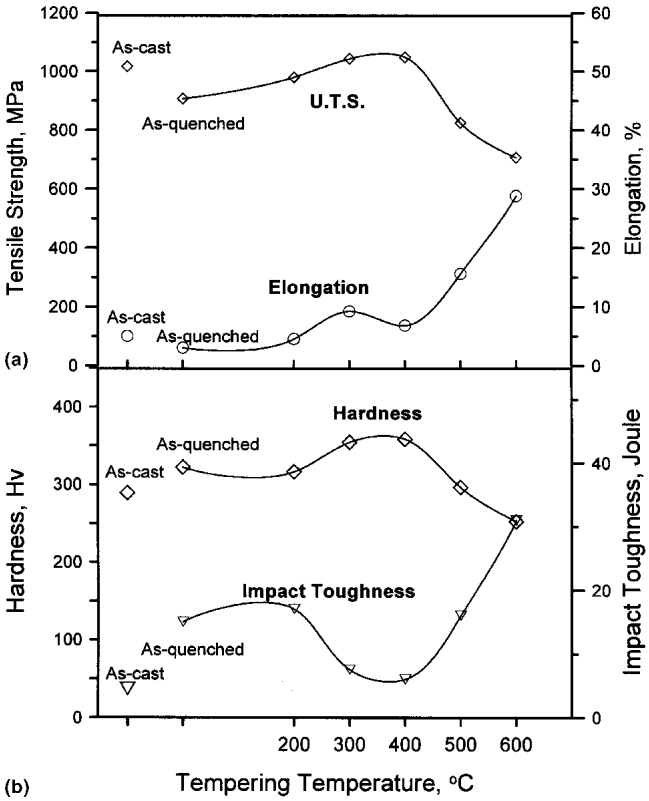

Fig. 3 Effect of the tempering treatment on the mechanical properties of the experimental material: **(a)** tensile strength and elongation; and **(b)** hardness and impact toughness

Table 1 Mechanical properties of the experimental materials

Heat treatment	Hardness, HV	UTS, MPa	Elongation, %	*E*, GPa	Impact toughness, J
As-cast	289	1017	5.0	206	4.5
As-quenched	322	907	10.5	148	15
Tempered					
200 °C	316	980	11.5	149	17
300 °C	354	1043	9.2	150	7.5
400 °C	358	1048	6.8	159	6
500 °C	296	824	15.6	168	16
600 °C	252	706	28.8	185	31

HV, Vickers hardness; UTS, ultimate tensile strength; *E,* elastic modulus

analyzed by emission spectroscopy as follows: Fe-0.14 C-0.34 Si-0.33 Mn-12.1 Cr-1.02 Ni-0.017 P-0.001 S. This chemistry conformed to the CA-15 nominal chemical specifications. Various specimens for mechanical testing and ultrasonic evaluation were machined from the cast plates and then were heat treated to different schedules. The heat treatment procedure involved austenitizing, quenching, and tempering, as shown in Fig. 1.

2.2 Mechanical Testing and Microstructural Analysis

Hardness testing of the samples was performed using a Vickers hardness tester (30 kg load). Five hardness readings were taken and averaged for each specimen. Tensile tests were carried out using a dynamic testing machine (MTS model 810 MTS Systems Corporation, MN). Specimens for tensile testing were machined according to the subsize tensile specimen of the ASTM E 8M standard.[12] Impact tests were carried out using a Charpy impact tester. Specimens for impact testing were machined according to the V-notch impact specimen of the ASTM E 23 standard.[13] Three tests were performed, and the results were averaged to represent the tensile strength, elongation, and impact toughness of the experimental material in each heat-treated condition.

Scanning electron microscopy (SEM), electron probe microanalysis (EPMA), and transmission electron microscopy (TEM) were used to examine the microstructure of the material. The specimens were polished and etched with Vilella's reagent (5 mL HCl + 1 g picric + 100 mL ethanol) for SEM and EPMA observations.

2.3 Ultrasonic Measurement

An ultrasonic A-scan pulsing instrument was attached to a gate monitor (model USIP12 with DTM 12 attachment, Krautkramer, Branson, PA) for ultrasonic measurement of the velocity, and for the first and second pulse peak amplitudes (i.e., the values $A1$ and $A2$ used in Eq 4) for attenuation coefficient calculations. Ultrasonic probes with frequencies of 1 and 5 MHz were used, and commercial motor oil was adopted as the coupling agent for the ultrasonic contact-type testing in these experiments. A longitudinal wave was propagated through the sample to evaluate the acoustic characteristics at the same position before and after heat treatments. Five ultrasonic readings of each specimen were taken and averaged to represent the data obtained.

3. Results and Discussion

3.1 Microstructure and Mechanical Properties

Microstructure of the experimental as-cast material mainly consisted of martensite and ferrite phases in the matrix along with chromium carbide films around grain boundaries (Fig. 2a). The carbide films were effectively eliminated by austenitizing at 1010 °C for 4 h followed by quenching, as shown in Fig. 2(b). Figure 2(c) shows the micrograph of the sample tempered at 400 °C. The microstructure was obviously unaltered, but the Cr content at the grain boundary of the martensitic phase had increased. Furthermore, ferrite islands started to precipitate in the martensite grains. After tempering at 500 and 600 °C, Cr and C were found to be uniformly dispersed in the matrix. Figure 2(d) shows micrographs of the sample tempered at 600 °C, at which point ferrite islands have precipitated in the martensite grains.

The mechanical properties of the material after different tempering treatments are listed in Table 1 and are illustrated in Fig. 3. After austenitization and quenching, the hardness and impact toughness were higher than those of the as-cast sample, but tensile strength was lower. The reason is that Cr carbides dissolve in the matrix for the austenitized specimens causing a hardness increase in the material. The increase of impact toughness resulted from the disappearance of boundary carbides, which could dominate the intergranular fracture in the

matrix. However, due to the boundary carbide effect and the retarded microcrack propagation being nonexistent, a reduction in tensile strength resulted. After tempering at 300-400 °C, secondary hardening/strengthening occurred for the material as a result of tiny carbides precipitating at the grain boundaries. These carbides can be seen clearly in the TEM micrographs (Fig. 4). This caused tempering martensite embrittlement (TME) and led to a reduction in impact toughness. After 500 and 600 °C tempering, the hardness and tensile strength of the material decreased, while the impact toughness increased, as a result of the softening of the matrix.

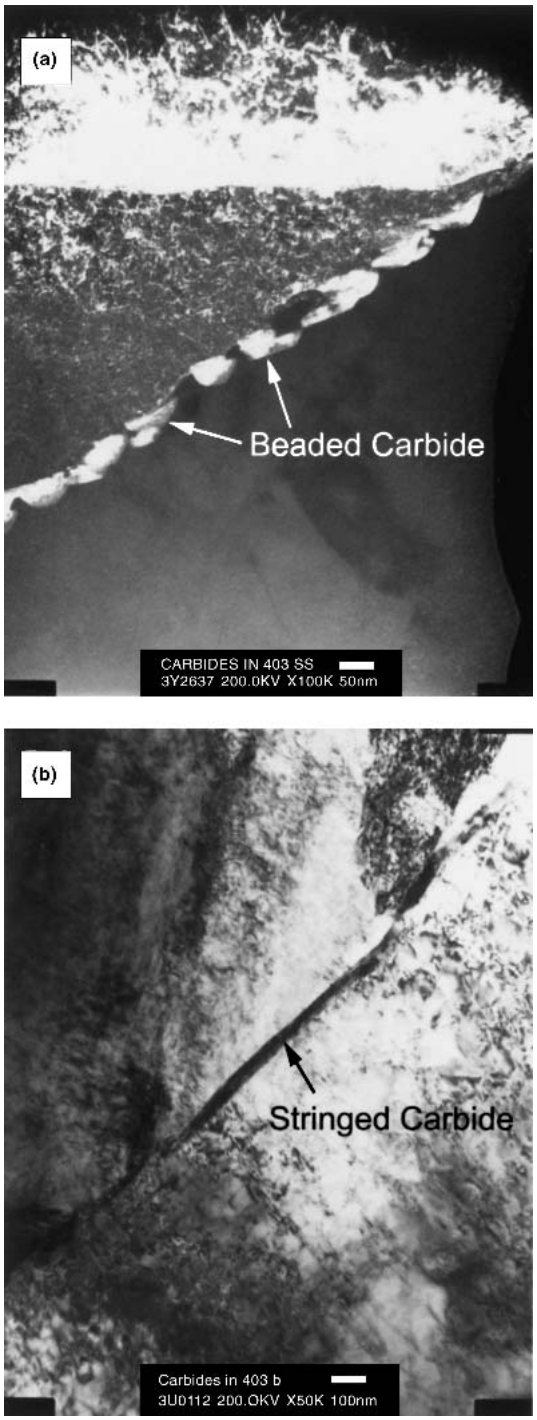

Fig. 4 TEM micrographs of the sample tempered at 400 °C: **(a)** beaded boundary carbide; and **(b)** stringed carbide

Table 2 Ultrasonic velocity and attenuation of the experimental materials

	1 MHz		5 MHz	
Heat treatment	**Velocity, m/s**	**Attenuation, dB/mm**	**Velocity, m/s**	**Attenuation, dB/mm**
As-cast	5912	0.07340	5889	0.15380
As-quenched	5879	0.04971	5877	0.12455
Tempered				
200 °C	5898	0.05146	5883	0.12419
300 °C	5916	0.05204	5891	0.13671
400 °C	5917	0.05017	5896	0.13441
500 °C	5928	0.04929	5898	0.12753
600 °C	5945	0.04673	5919	0.10899

3.2 Interrelation of Ultrasonic Velocity and Mechanical Properties

The ultrasonic characteristics from various tempered specimens are listed in Table 2. Figure 5(a-d) illustrates the relationship between ultrasonic velocity and mechanical properties. From these figures, it is clearly seen that the data were quite scattered and that no particular relationship exists among ultrasonic velocity hardness, toughness, or tensile strength. However, it is interesting that there was a distinct positive correlation (correlation coefficient >0.85) between the ultrasound velocity and the E of the specimens (except for the as-cast sample). These results are shown in Fig. 6. The E of the material was changed by tempering treatments, and the ultrasonic velocity increased with an increase in E. Also, the as-cast sample possesses a higher value of E than that of the tempered samples and results from the carbide films at the grain boundaries retarding the elastic deformation of the material in the linear elastic strain region.

Incidentally, for detection with the 1 MHz probe, the variation of ultrasonic velocity was similar to that of the 5 MHz probe. However, the ultrasonic velocity at 1 MHz was higher than that at 5 MHz. The reason for this is yet unknown.

3.3 Interrelation of Ultrasonic Attenuation and Mechanical Properties

Figure 7 depicts the relationship between the ultrasonic attenuation coefficient α and the mechanical properties. The as-cast specimen showed substantial acoustic attenuation compared with the heat-treated specimens, and this might have resulted from the carbide films at the grain boundaries causing a scattering of the acoustic wave. Therefore, despite the anomalous behavior of the as-cast specimen, linear equations were derived and are shown in Fig. 7. It can be clearly seen that strength and hardness are positively correlated with the attenu-

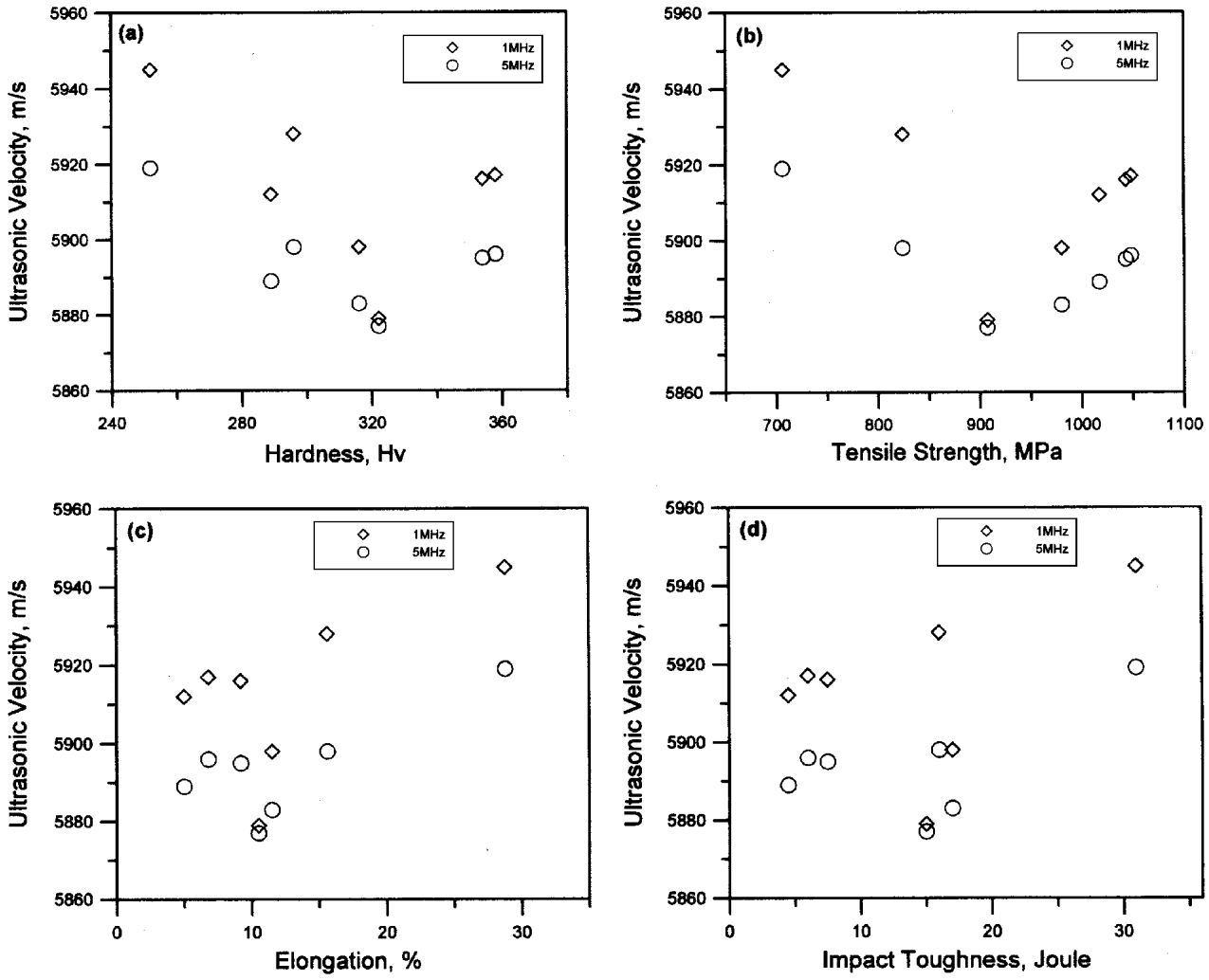

Fig. 5 Relationship between the ultrasonic velocity and the mechanical properties of the experimental materials, under different frequencies: **(a)** hardness; **(b)** tensile strength; **(c)** elongation; and **(d)** impact toughness

ation coefficient, while toughness and elongation are negatively correlated with it. Correlation coefficients of all the linear equations were >0.8. This correlation implies that the attenuation coefficient plays an important role in evaluating the mechanical properties of the material. Table 3 shows the correlation equations for relationships between the ultrasonic attenuation coefficient and various mechanical properties and provided the formula for the evaluation of mechanical properties based on the nondestructive ultrasonic attenuation data. In addition, the higher the ultrasonic frequency, the higher the attenuation coefficient obtained. However, it also resulted in greater scatter of the attenuation data.

4. Conclusions

The purpose of this research was to derive relationships among the ultrasonic characteristics and mechanical properties of tempered CA-15 MSS. The following conclusions can be made:

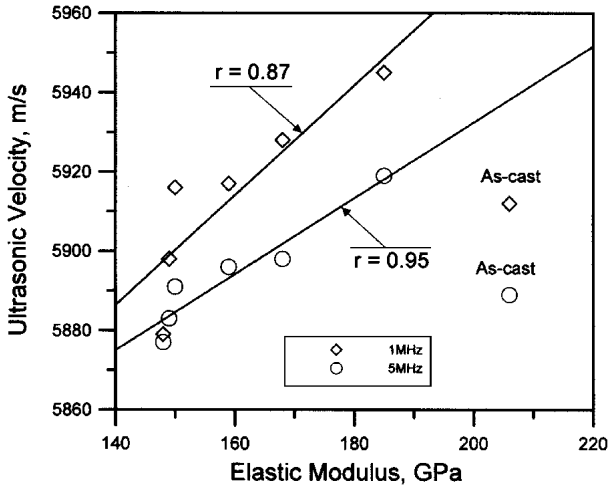

Fig. 6 Relationship between the ultrasonic velocity and the E of the experimental materials, under different frequencies (r is the correlation coefficient)

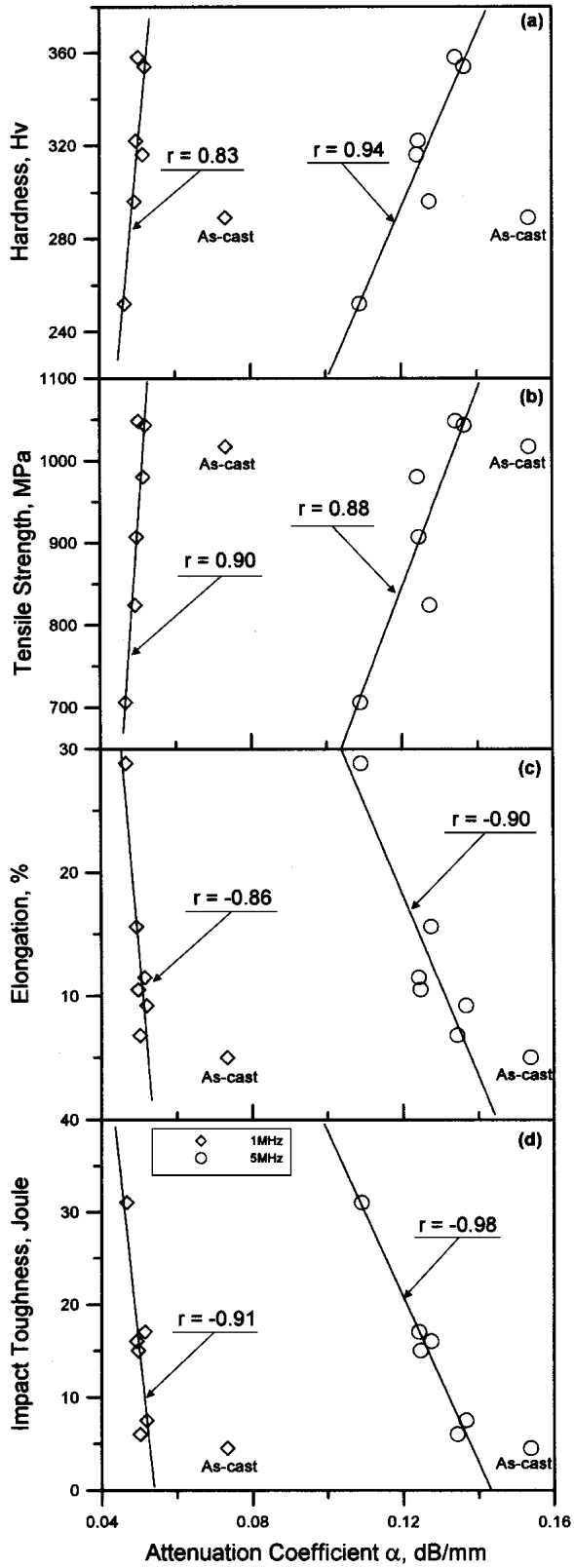

Fig. 7 Relationship between the ultrasonic attenuation and the mechanical properties of the materials, under different frequencies: **(a)** hardness; **(b)** tensile strength; **(c)** elongation; and **(d)** impact toughness (*r* is the correlation coefficient)

Table 3 Correlation equations of attenuation coefficient and mechanical properties using different frequencies

Probe frequency	1 MHz	5 MHz
Hardness, HV	$Y = 17{,}401X - 552$	$Y = 3757X - 157$
Tensile strength, MPa	$Y = 64{,}277X - 2289$	$Y = 12{,}039X - 600$
Elongation, %	$Y = -4156X + 2198$	$Y = -680X + 97$
Impact toughness, J	$Y = -3788X + 204$	$Y = -893X + 128$

Note: *X,* attenuation coefficient; *Y,* mechanical properties

- The microstructure of the material consisted mainly of martensite and ferrite with carbide films around the martensite interphase boundaries. These carbide films retarded microvoid propagation (i.e., increased the strength) during tensile testing but caused grain boundary embrittlement (i.e., reduced the toughness) during impact testing and distinctly scattered and attenuated the propagated acoustic waves.
- The ultrasonic velocity of the wave in the samples, except for the as-cast material, was positively correlated with the *E*. The relationship between the ultrasonic velocity and the mechanical properties was not obvious.
- The attenuation coefficient was positively correlated with the strength and the hardness of the material, but was negatively correlated with the toughness and elongation.
- For ultrasonic characteristic evaluation, the higher frequency (5 MHz) probe, compared with the 1 MHz probe, had better sensitivity, a higher attenuation coefficient (α), and a lower velocity value. However, using this probe resulted in relatively dispersed data.

Acknowledgment

The authors wish to thank the National Science Council (Taiwan) for financial support for this research under project NSC89-2216-E-036-020.

References

1. Properties and Section: Irons, Steels, and High-Performance Alloys, 10th ed. *ASM Handbook* Vol 1, ASM, 1990, p 908-929
2. O. Prabhakar, R. Ambardar, and H.K. Wah, Percentage Porosity Measurement by a Through-Transmission Ultrasonic Technique, *Insight,* Vol 39 (No. 2), 1997, p 100-103
3. R. Ambardar, M.T. Muthu, S.D. Pathak, and O. Prabhakar, Effect of Porosity, Pore Diameter and Grain Size on Ultrasonic Attenuation in Aluminum Alloy Castings, *Insight,* Vol 37 (No. 7), 1995, p 536-543
4. S.M. Nair, D.K. Hsu, and J.H. Rose, Porosity Estimation Using the Frequency Dependence of the Ultrasonic Attenuation, *J. Nondestr. Eval.,* Vol 8 (No. 1), 1989, p 13-26
5. L. Adler, J.H. Rose, and C. Mobley, Ultrasonic Method to Determine Gas Porosity in Aluminum Alloy Castings: Theory and Experiment, *J. Appl. Phys.,* Vol 59 (No. 2), 1986, p 336-347
6. A.D. Degtyar, A.I. Lavrentyev, and S.I. Rokhlin, New Method for Determination of Applied and Residual Stresses in Anisotropic Materials From Ultrasonic Velocity Measurement, *Mater. Eval.,* Vol 55 (No. 10), 1997, p 1162-1168
7. E.P. Papadarkis, Revised Grain-Scattering Formulas and Tables, *J. Acoust. Soc. Am.,* Vol 37 (No. 4), 1965, p 703-710
8. R.L. Smith, The Effect of Grain Size Distribution on the Frequency

Dependence of the Ultrasonic Attenuation in Polycrystalline Materials, *Ultrasonics,* Vol 9, 1982, p 211-214
9. R. Klinman, G.R. Webster, F.J. Marsh, and E.T. Stephenson, Ultrasonic Prediction of Grain Size, Strength, and Toughness in Plain Carbon Steel, *Mater. Eval.,* Vol 38 (No. 10), 1980, p 26-32
10. D. Leviston and B. Bridge, Evaluation of the Subsurface Microstructure of Quenched and Tempered Carbon Steel by Ultrasonic Backscatter, *NDT Int.,* Vol 21 (No. 1), 1988, p 17-25
11. J. van den Andel, *Nondestructive Testing Handbook: Ultrasonic Testing,* Vol 7, P. Mclntire, Ed., ASNT, 1991, p 830-850
12. "Standard Test Methods for Tension Testing of Metallic Materials," E 8M, *Annual Book of ASTM Standards,* Section 3, Vol. 03.01, ASTM, 1997, p 77-97
13. "Standard Test Methods for Notched Bar Impact Testing of Metallic Materials," E 23, *Annual Book of ASTM Standards,* Section 3, Vol. 03.01, ASTM, 1996, p 137-156